Wind Energy

WIND ENERGY
Wind Energ. 2016; **19**:1687–1697
Published online 6 November 2015 in Wiley Online Library (wileyonlinelibrary.com). DOI: 10.1002/we.1944

RESEARCH ARTICLE

Demonstrating the effect of vertical and directional shear for resource mapping of wind power

Christopher T. M. Clack[1,2], Anneliese Alexander[1,2], Aditya Choukulkar[1,2] and Alexander E. MacDonald[2]

[1] Cooperative Institute for Research in Environmental Sciences (CIRES), University of Colorado, Boulder, Colorado, USA
[2] National Oceanic and Atmospheric Administration (NOAA), Boulder, Colorado, USA

ABSTRACT

The use of wind energy is growing around the world, and its growth is set to continue into the foreseeable future. Estimates of the wind speed and power are helpful to assess the potential of new sites for development and to facilitate electric grid integration studies. In the present paper, wind speed and power resource mapping analyses are performed. These resource mappings are produced on a 13 km, hourly model grid over the entire continental USA for the years of 2006–2014. The effects of the rotor equivalent wind speed (REWS) along with directional shear are investigated. The total dataset (wind speed and power) contains ≈152,000 model grid points, with each location containing ≈78,000 hourly time steps. The resource mapping and dataset are created from analysis fields, which are output from an advanced weather assimilation model. Two different methods were used to estimate the wind speed over the rotor swept area (with rotor diameter of 100 m). First, using a single wind speed at hub height (80 m) and, second, the REWS with directional shear. The demonstration study shows that in most locations the incorporation of the REWS reduces the average available wind power. In addition, the REWS technique estimates more wind power production at night and less production in the day compared with the hub height technique; potentially critical for siting new wind turbines and plants. However, the wind power estimate differences are dependent on seasonality, diurnal cycle and geographic location. More research is warranted into these effects to determine the level at which these features are observed at actual wind plants. © 2015 The Authors. *Wind Energy* published by John Wiley & Sons, Ltd.

KEYWORDS
wind power; numerical weather prediction; power modelling; wind shear; rotor equivalent wind speed; renewable energy; datasets; techniques; data assimilation

Correspondence
Christopher T. M. Clack, CIRES, University of Colorado at Boulder, 325 Broadway, Boulder, Colorado 80305, USA.
E-mail: Christopher.Clack@NOAA.gov

This is an open access article under the terms of the Creative Commons Attribution-NonCommercial License, which permits use, distribution and reproduction in any medium, provided the original work is properly cited and is not used for commercial purposes.

Received 29 September 2014; Revised 2 October 2015; Accepted 11 October 2015

1. INTRODUCTION

The increasing threat of anthropogenic climate change is creating a shift in the way energy is provided. The fastest growing industry within the electricity sector is wind energy, and this is set to continue until at least 2050,[1,2] because it is one of the cheapest forms of alternative energy.[3] The radical change in energy production has borne a field of research in the mapping of the resources available (e.g. Potter *et al.*).[4] One important criteria for a good wind resource site is the amount of wind energy available for power production. However, many other factors contribute to determine if a site should be developed. We will only consider the resource in terms of the wind power availability.

Significant research effort has been applied to wind resource mapping (via reanalysis or weather model forecast output) along with the possible overestimation of resource mapping due to limitations of wind power extraction [e.g. Bailey *et al.*; Archer L. and Jacobson M. (2005) ; Adams A S., Keith D W. (2013); Archer C L, Jacobson M Z. (2013)].[5–8] The majority of past wind resource mappings have relied on hub height wind speeds from some form of numerical weather prediction models.[9,10] These resource mappings are then utilized to make decisions about policy, system design and economics. It is therefore critical that the resource mapping be as accurate as possible. An alternative to computationally expensive dataset

is to use simplistic probabilistic estimations; variants of this method have been studied extensively in the literature.[11–16] As discussed by Zhou F. and Smith S J. (2013),[17] however, these distributions lack accurate hourly data at high geographic resolution that are needed for true planning purposes. The present study aims to address a main deficiency of past research by using hourly analyses from an advanced weather assimilation model to produce a 13 km gridded resource mapping and dataset for 9 years (2006 − 2014).

The present paper tries to reduce the error in grid cell averaged wind power estimates by applying the rotor equivalent wind speed (REWS) and by incorporating directional shear. The REWS procedure computes the weighted average of wind speeds at different heights over the rotor diameter. The directional shear takes into account the drift in wind direction that is possible over the rotor swept area. The computations are approximations, allowing both wind speed shear and directional shear to be accounted for within the wind power estimate. The incorporation of the wind speed and directional shear provides more information about the atmosphere interacting with the wind turbines. Thus, seeking for help reduce the risk of financial hardship for plant operators and planners. The REWS will be applied to the analyses fields from an advanced weather assimilation model for the first time over such a large geographic and temporal extent. The REWS concept was originally developed and used with measurements by.[18] It has recently been extended and applied to LiDAR data by Choukulkar *et al.*[19]

The demonstrated techniques in the present paper will be applied to higher resolution models and compared against wind farm power data in forthcoming papers. The scope of the present paper is to show the effects of the REWS on the power estimates at coarse resolution to give a first approximation and to highlight areas of particular interest. The paper is organized as follows: in Section 2, we briefly describe the methodology of REWS and the data we use; Section 3 displays the results of the work; and Section 4 contains the discussions and conclusions for the present work, along with the future avenues of investigation.

2. METHODOLOGY

2.1. Hub height wind speed versus rotor equivalent wind speed

Typically, to produce an estimate of wind power, only one wind speed is calculated: the wind speed at the hub height. The current paper assumes a hub height of 80 m above ground level (AGL), along with a rotor diameter of 100 m. These values are chosen because they are the most typical values found across the contiguous USA.[20] It is known that the wind speed changes with height, and so the estimate of the wind speed at the hub height alone does not represent how the wind speed varies over whole rotor diameter for different conditions, e.g. stability conditions. The REWS, e.g. Wagner *et al.*, Choukulkar *et al.*,[18,19] provides a solution to overcome this deficiency. The REWS can also incorporate the directional shear, which will be discussed later.

The data utilized in the present paper is obtained from the 13 km rapid update cycle (RUC) advanced assimilation model.[21,22] The RUC assimilation model uses in excess of 20,000 observations each hour in combination with a one hour forecast, from the previous model cycle, to obtain an analysis field for the state of the atmosphere. The assimilation analysis balances the large number of observations and the short term model forecast to minimize the errors from the data and the model; essentially creating the best possible estimate of the current state of the atmosphere. The assimilation data collected has 13 km hourly resolution and encompasses the nine years of 2006–2014. The full three dimensional matrices are collated and stored. They are saved for use in wind speed estimates at specific AGL heights and wind power modelling. The spatial resolution of the RUC provides 151,987 geographic locations across the contiguous USA for the dataset. Further, each geographic site contains 74,283 hourly time steps of data. The missing data (5.8%) was due to incomplete cycling from when the model was originally run. The native levels of the RUC are in the hybrid isentropic-sigma coordinate, facilitating benefits from both terrain following and entropy conserving coordinates.[21] The wind vectors computed by the RUC assimilation model are output on its native levels and in component form. The components can be combined to produce the horizontal wind speed at each native level (U_η),

$$U_\eta = \sqrt{u_\eta^2 + v_\eta^2} \tag{1}$$

where η is each of the native model levels, u is the East–West component and v is the north–south component. Because the native levels are not constant in height AGL, we have to interpolate U_η to specific heights, such as the hub height of 80 m. The original U_η are stored for future work at different hub heights.

For the present work, the rotor swept area is divided into 10 m vertical slices (segments). Following the work by, Wagner *et al.*[18] the REWS can be defined as

$$U_R = \sum_{i=1}^{N} \alpha_i \cdot U_i, \text{ where } \alpha_i = \frac{A_i}{A} = \frac{(\theta_i - \sin\theta_i)}{2\pi} - \frac{1}{A}\sum_{j=0}^{i-1} A_j, \quad i \geq 1 \tag{2}$$

Wind Energ. 2016; **19**:1687–1697 © 2015 The Authors. *Wind Energy* published by John Wiley & Sons, Ltd.
DOI: 10.1002/we

In equation (2), U_R is the REWS, U_i is the wind speeds at different heights across the rotor diameter, θ_i is the angle to the chord of the top of the vertical slice being computed and A_i/A is the weighted area of the rotor swept area. The definition of the REWS from equation (2) remains valid as long as the rotor diameter is not larger than the horizontal resolution of the model (here they are not). The limit of the REWS is a continuous function of wind speed integrated over the rotor height. If the resolution of the model were to be so high that the rotor diameter is greater than the horizontal grid spacing, then the REWS would need to be recomputed using both horizontal and vertical slices. The ultimate limit to the REWS would be the double integral of continuous wind speeds over the entire rotor swept area.

In addition to the vertical wind speed shear, we wish to add the directional shear. Instead of simply taking U_i as the horizontal wind speed at each height, we calculate the projection of the horizontal wind speed at each height that is parallel to the wind direction at hub height. In doing so, we assume that the nose of the turbine nacelle is aligned exactly to the direction of the wind at hub height. Therefore, we define U_i as

$$U_i = \frac{u_i \cdot u_H + v_i \cdot v_H}{U_H} \tag{3}$$

where the subscript H denotes the variable computed at hub height and the lower case represents the component vectors of wind speed.

The purpose of calculating the REWS, with directional shear, to estimate wind power, is to provide more information from the state of the atmosphere. The hypothesis is that more information should improve the estimates in terms of behaviour and magnitude. We are applying the REWS to numerical weather assimilation data over a vast geographic area, something not addressed in the literature thus far.

2.2. Wind power modelling

The full production of wind speed estimates is complex and requires multi-disciplinary analysis. However, we circumvented the majority of the work required to produce wind speed estimates because we obtained the historical data from the archives of the RUC assimilation model.[21] Our work focuses on the production of the REWS with directional shear and wind power estimates. To produce wind power estimates for wind turbines, we must know how power in the wind is expressed.

The energy content of the wind in a volume is simply the kinetic energy ($mv^2/2$) of the wind contained within that volume. Hence, the power contained in the wind is the time derivative of the kinetic energy;

$$P_w = \frac{d[E_w(U(t))]}{dt} = \frac{d}{dt}\left[\frac{1}{2}\cdot A\cdot \rho(t)\cdot L(t)\cdot U^2(t)\right] = \frac{\rho A U^3}{2}\left[1 + \left(\frac{\int U\,dt}{U}\right)\left(\frac{1}{\rho}\frac{d\rho}{dt} + \frac{2}{U}\frac{dU}{dt}\right)\right] \tag{4}$$

Here, A is the cross section area normal to the direction of the wind, ρ is the density of the air, L is the length of the volume in the direction of travel of the wind and U is the horizontal wind speed over the cross sectional area. If we assume the wind speed and density do not change with time, we recover the well-known equation for wind power[23]

$$P_w = \frac{1}{2}C_p \rho A U^3 \tag{5}$$

Here, the C_p represents the coefficient of power (an empirically derived curve from simulations and performance of individual turbines), which is the ratio of the electric power created by the wind turbine divided by the power available in the wind ($C_p = P_t/P_w$). The right hand side terms in equation (4), which become zero when considering instantaneous power, are related to fluctuations in the density and wind speed; but are proportional to the discretization time scale. For the present paper, we assume these terms are small compared with the first term. However, it is noted by the authors that these additional terms could be non-negligible in steep ramp conditions, or long integration periods.

To calculate the wind power estimates, we replace U in equation (5) with U_H for the hub height version, and U_R for the REWS version. We require the coefficient of power as an input. It is assumed that the same C_p curve can be used for both hub height wind speeds and rotor equivalent wind speeds. For the present paper, we take the composite of three or four specific turbines for each of the International Electrotechnical Commission (IEC) classes I, II, III and offshore, and back calculate the C_p curves.[24,25] The turbines used are found in Table I. The C_p curves and their corresponding normalized power curves are shown in Figure 1. Above 25 m s^{-1}, all turbines shutdown, and power drops to zero. At peak efficiency, the turbines are approaching 50% extraction of the available wind power, which is approximately 85% of the theoretical maximum (59%) possible for wind turbines.[26]

As stated earlier, we use the same rotor diameter for all of the IEC classes. If we had used different rotor diameters for each class, the REWS would be computed differently for the four classes making comparisons more difficult. Because of the 100 m rotor diameter, the rated power for each class is different; IEC–I is 3.2 MW, IEC–II is 2.5 MW, IEC–III is 2.0 MW and offshore is 3.5 MW. These values are utilized to normalize the power output for the dataset (so that all data lies between 0 and 1). To define each RUC grid cell IEC class, we minimized the difference between the computed 9 year mean hourly wind speed at 80 m AGL and the average wind speed in IEC-61400-1.[27] Offshore locations are designated

Table I. Turbines used to calculate the generic coefficient of power curves for the IEC classes.[24,25]

	Turbine	Rated power (MW)	Cut-in speed (m s^{-1})	Max output speed (m s^{-1})	Cut-out speed (m s^{-1})	Rotor diameter (m)
IEC–I	Siemens 3.0 MW	3.0	3.0	14.0	25.0	101.0
	Gamesa G80	2.0	4.0	17.0	25.0	80.0
	Nordex N90HS	2.5	4.0	14.0	25.0	90.0
	Vestas V90	3.0	4.0	14.0	25.0	90.0
IEC–II	Vestas V112	3.0	3.0	13.0	25.0	112.0
	Siemens 2.3 MW	2.3	3.0	13.0	25.0	93.0
	GE1.6 82.5	1.6	4.0	12.0	25.0	82.5
	GE2.5xl	2.5	3.0	14.0	25.0	100.0
IEC–III	Vestas V100	1.8	3.0	12.0	20.0	100.0
	GE1.6-100	1.6	3.0	12.0	25.0	100.0
	Repower 3.2M	3.2	3.0	12.0	22.0	114.0
Offshore	Siemens 3.6 MW	3.6	4.0	14.0	25.0	107.0
	GE4.1MW	4.1	4.0	14.0	25.0	113.0
	Repower 6M	6.15	3.5	14.0	30.0	126.0

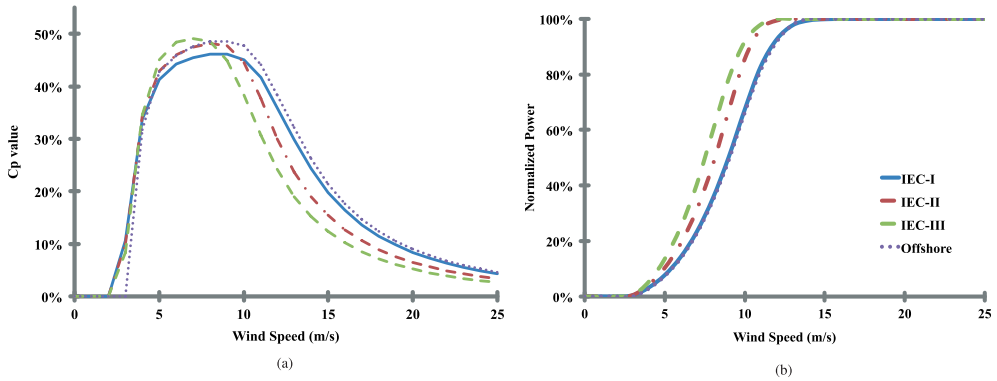

Figure 1. (a) The coefficient of power and (b) the normalized power curves for four generic IEC wind classes.

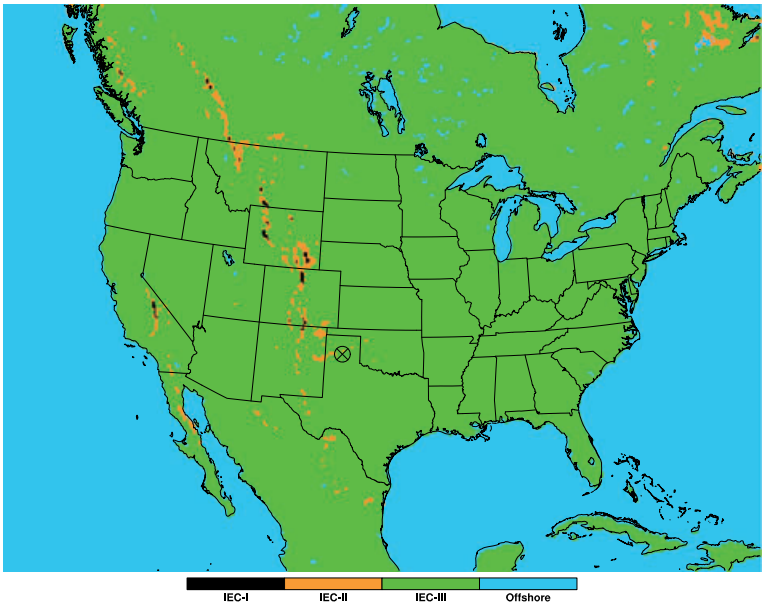

Figure 2. The classification of RUC grid cells using the mean wind speed at 80 m AGL. The black is IEC–I, orange is IEC–II, green is IEC–III and blue is offshore. The cross in north Texas denotes the site of a tall tower used for verification.

Wind Energ. 2016; **19**:1687–1697 © 2015 The Authors. *Wind Energy* published by John Wiley & Sons, Ltd.
DOI: 10.1002/we

using the RUC land/sea mask. The defined classifications can be seen in Figure 2. The US is predominantly IEC-III, with small areas of IEC–II, and even fewer locations of IEC-I. The location of the IEC–I and II classes are strongly correlated with steep terrain.

To create the dataset of wind power estimates for the 9 years of 2006–2014, we created an algorithm that passed the wind speeds (U_H and U_R) and density for each grid cell through equation (5). For the REWS power estimates, a rotor equivalent density, a rotor equivalent temperature, and a rotor equivalent clouds were calculated for each grid cell in the same manner as the REWS. We set conditions for turning off the turbines within the algorithm that are related to icing. The icing constraints are applied homogeneously across the whole model grid space. First, if the temperature (at hub height or the rotor equivalent temperature) is below −20°C the turbine is deactivated. Second, if the temperature is below 0°C, and there are clouds within the rotor swept area the turbine is deactivated. Third, if the temperature is below −5°C and there is precipitation falling the turbine is deactivated. The algorithm carries out the exact same procedure for every RUC grid cell, i.e. there are no localized constraints.

3. RESULTS

Using the techniques described in Section 2, we produced a 9 year (2006 − 2014) demonstration (13 km, hourly resolution) wind speed and power dataset. Figure 3 displays the 9-year grid cell averaged mean hourly REWS for the entire RUC domain.

We show Figure 3 to facilitate some comparison with the AWS True Power with National Renewable Energy Laboratory (AWS/NREL) 80 m average wind speed map (http://www.nrel.gov/gis/wind.html). The AWS/NREL map is produced at a spatial resolution of 2 km, therefore more detail is expected. Overall, Figure 3 and the AWS/NREL maps look remarkably similar. The plains enclose the greatest resource, with the face of the Rockies having some of the highest mean wind speeds. The comparison highlights the benefit of using a Numerical Weather Prediction (NWP) model with a hybrid coordinate; the 13 km map has the ability to recognize terrain features (and speed up effects) that are also seen in the 2 km AWS/NREL map. For example, the semi circular ridge that runs north–south in northern Wyoming, with a low wind resource region to its east and west, is resolved with similar mean wind speeds as the AWS/NREL map. Figure 3 covers a larger geographic area than the AWS/NREL map, showing large portions of Canada and significant offshore resources. The AWS/NREL map shows significantly more detail in the western half of the USA because of its additional resolution. From qualitative

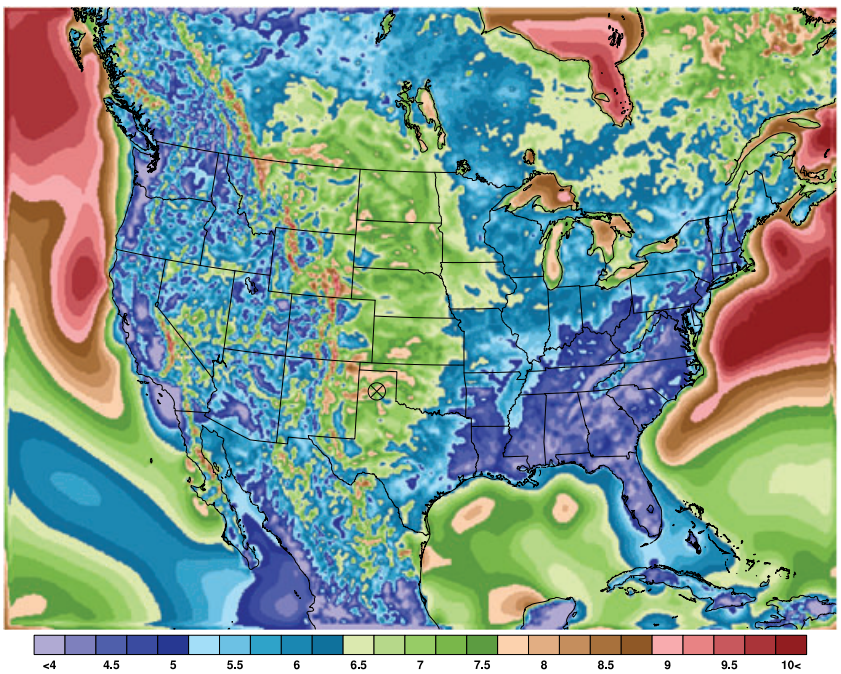

Figure 3. The 2006 − 2014 mean rotor equivalent wind speeds for each RUC grid cell. The mean REWS is given in m s^{-1}. The map shows the grid cell average hourly REWS calculated from data over 9 years, which is typically half the investment period of a wind plant. The circled cross indicates the location of a tall tower in Washburn, TX that has publicly available data.

comparison with the AWS/NREL wind resource map at 80 m AGL, it can be seen that the REWS does not appear to alter the highest quality wind resource locations.

The current paper is a demonstration of estimating wind power using NWP analysis fields to estimate the REWS with directional shear. It is instructive to compare the wind speed estimates from the RUC and observations. We found publicly available data from a tall tower that measures wind speeds at 100 m AGL in Washburn, TX (http://www.windenergy.org/datasites/52-talltowernorth/). It has a long term record of hourly wind speeds. We estimate the 100 m AGL wind speeds from the RUC grid cell that is closest to the tall tower. The comparison between the observed wind speeds and the estimated wind speeds is shown in Figure 4. Figure 4(a) shows that the modelled wind speed slightly over predicts at low wind speeds (< 7 m s^{-1}) and slightly under predict at high wind speeds. The measured average hourly wind speed at the Washburn, TX site for 2006 – 2011 is 9.0 m s^{-1}. For the majority of the power producing portion (> 7 m s^{-1}) of wind speeds, the RUC grid cell averaged 100 m AGL wind speed has a low bias.

In Figure 4(b), a time series comparison between the RUC and the observations can be seen. The time series is the hourly values for the first 7 days of 2006. The model follows the pattern of the wind speeds very well, with the notable exception of the third day. It should be noted that the RUC estimated 100 m AGL wind speed is a grid cell average over $\sim$169 km^2, while the observations are a single points; therefore we would not expect an exact match. The bias for the Washburn, TX site remains around -0.80 m s^{-1}) each year, and so the RUC assimilation model does not appear to improve for wind speed estimates over the time horizon analysed. The site is situated on a slightly sloped, elevated plateau that is right on the edge of a transition region, between very good wind resource on the plateau ($\sim$8.5 m s^{-1}) and moderate wind resource to the north and south due to river valleys ($\sim$6.5 m s^{-1}). The validation against the tall tower in Washburn, TX indicates that the model can reproduce the wind speeds at 100 m at hourly resolution with reasonable accuracy. Since the scope of the current paper is to demonstrate and highlight the coarse effects of the REWS, we do not compare the wind speeds to multiple other sites. We plan a future paper that aims to look at many more sites to compute statistics, and possibly a bias correction method to further improve the wind speed accuracy.

Figure 5 displays the 9-year average capacity factors over the entire RUC domain for the REWS estimated wind power (Figure 5(a)) and the percentage difference with the hub height estimated wind power (Figure 5(b)). The difference is calculated as the percentage of energy added or lost, compared with the hub height wind speed estimate. The capacity factor map shows the commonly seen features across the USA, such as the majority of the southeast having low capacity factors (<20%). The regions that overlap with that created by the Midcontinent Independent System Operator (MISO) energy (www.misoenergy.org/WhatWeDo/StrategicInitiatives/Pages/WindCapacity.aspx) can be compared and can be seen to be in very good agreement. For example, the split ridge starting on the north border of South Dakota that continues into southern Minnesota aligns very well. Unfortunately, not many capacity factor maps are available in the literature to do direct comparisons, because most resource maps are created in wind speed form rather than capacity factor. However, with the qualitative comparison with the AWS/NREL wind mapping and the MISO capacity factor mapping along with the quantitative comparison with the Washburn, TX site, there are indications that the REWS approach is robust; in that, it does not drastically alter the positioning or average energy production in less sheared environments.

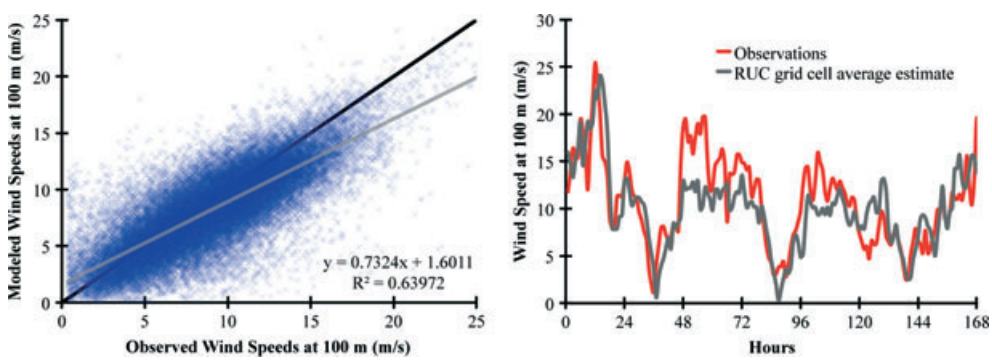

(a) (b)

Figure 4. (a) Scatter comparison between hourly 100 m AGL wind speeds from publicly available data at a tower data in Washburn, TX and the RUC grid cell averaged 100 m wind speed estimate. The location of the Washburn, TX site is indicated in all the maps by a circled cross. The public data is only available up to the end of 2011. Each blue cross is a datapoint pair. The grey line is the least squares correlation from the data. Each individual year showed the same overall relationship and a similar bias. The mean bias error is -0.80 m s^{-1}, and the root mean squared error is 2.47 m s^{-1}. (b) The 100 m AGL wind speeds time series for the first 7 days of 2006 are shown. Red is the observations, and dark grey is the RUC grid cell average.

Wind Energ. 2016; **19**:1687–1697 © 2015 The Authors. *Wind Energy* published by John Wiley & Sons, Ltd.
DOI: 10.1002/we

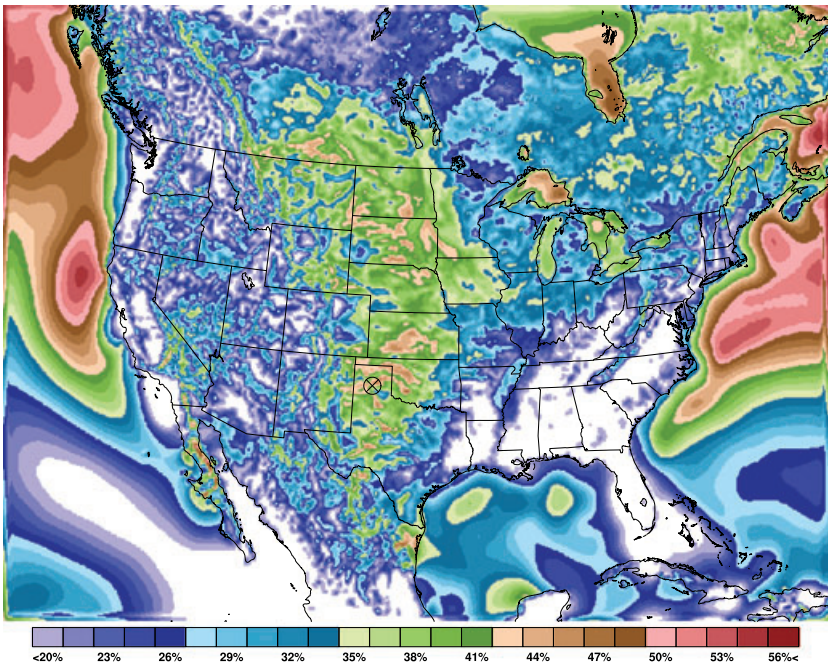

(a)

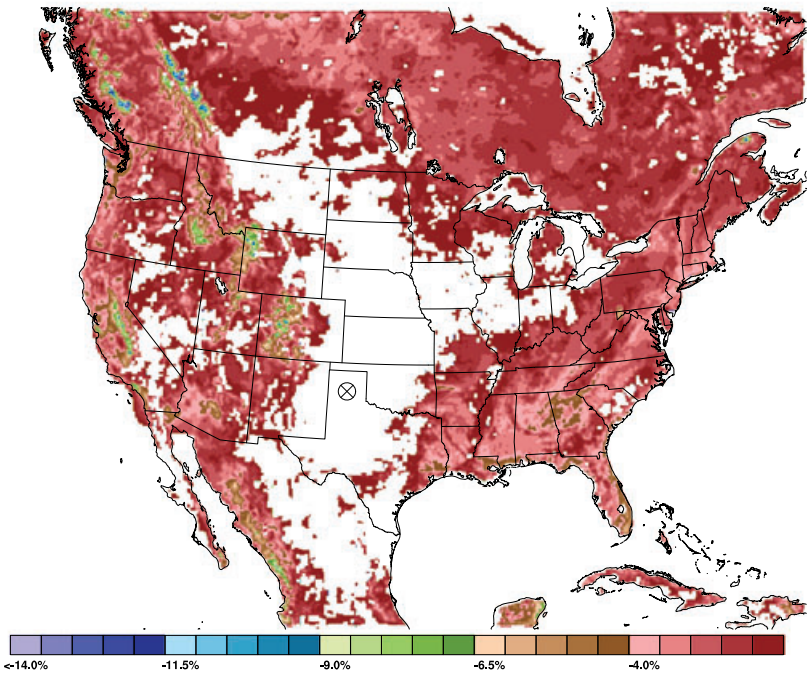

(b)

Figure 5. (a) The 9-year grid cell averaged capacity factor (%) for the entire RUC domain using the REWS with directional shear at 80 m AGL and 100 m rotor diameter. \Capacity factors lower than 20% are transparent. The C_p curve, density and the cube of the wind speed contribute to the power estimates. (b) The 9-year difference (%) in potential energy with a reduction of greater than 1%. The largest reductions are in areas of complex terrain. The high resource region of the great plains shows little difference in comparison with the hub height estimated potential energy over 9 years.

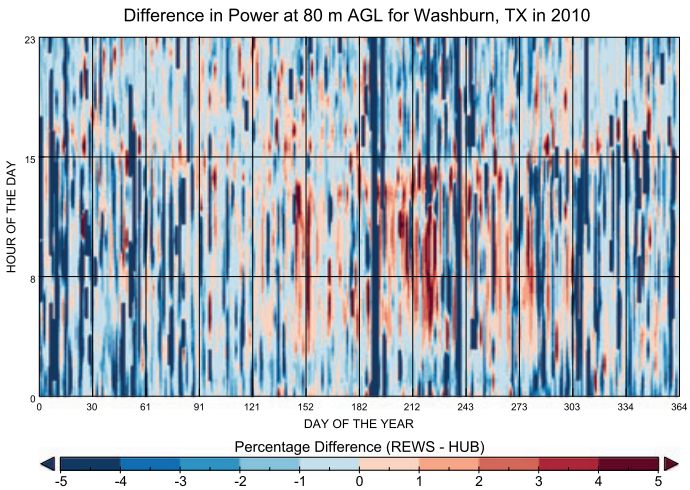

Figure 6. Hourly difference heat map for the Washburn, TX site between the REWS estimated power and the hub height estimated power for 2010. The horizontal axis is for days of the year (each vertical line is 31 days), and the vertical axis is hour of the day in UTC. Red indicates an increase in estimated power, and blue denotes a reduction in estimated power. An annulus of increased power can be seen at both sunrise and sunset (less defined) times. The summer months show a strong increase in power over the night time hours. Predominantly, less power is estimated during the day time, but higher power is estimated sporadically during the spring and fall morning to afternoon. All years exhibit similar behaviours.

In Figure 5(b), it is seen that the REWS estimated power over the 9 years barely changes the energy potential in the great plains (<1%). As an example, the difference for the Washburn, TX site is −0.6% over the 9 years. The largest differences can be found in steep terrain settings, which is expected beccause of increased shear. The largest difference was found on the eastern edge of the rocky mountains in Canada at −15.4%. The average over the whole domain was a reduction of −1.56%. The REWS reduces the average energy available at 80 m AGL compared with the hub height estimate. The difference at a specific location due to the REWS will depend on the particular environment. When analysed by season, the great plains continue to have small differences compared with the hub height estimates, but all other regions experience changes depending on the season. The eastern states have much larger reductions (−5 to −7%) in the summer months than the other months (−1 to −2%).

In Figure 6, the heat map of hourly differences illustrates a number of interesting features of the REWS estimates versus the hub height estimate. First, even though the annual (and season) averaged differences are small (<1%), the time series for the REWS is significantly altered from the hub height version; with consequences for planners and operators. Second, there is generally an increase in power in the REWS around sunrise and, to a lesser extent, sunset. Third, the night time in summer exhibits regular increased power estimates; this could be due to the low level jet that occurs in this region. Fourth, the power estimate is generally lower in the day time hours. Fifth, in the spring and fall, a more complex picture emerges, in that both higher and lower power production is estimated; likely due to convection activity. Overall, there is more production at night (even more so in summer) and less production during the day when considering the REWS. Other randomly selected sites also exhibit this behaviour but not always to the same extent.

To be able to use a dataset for planning purposes, or dispatching and integration studies, the time series must incorporate as much information as possible with regard to the power estimates at possible generation sites. With a relatively simple addition to the way the power is estimated (including vertical wind speed and directional shear), there are significant changes to the time series behaviour. Further research is warranted to determine if the vertical shear is an appropriate addition to the power estimates, and if the difference behaviour is replicating reality. Other researchers have performed some research, which suggests that vertical shear is an important component for wind power estimates, see e.g.,[18,19,28–31] but the present paper is the first in the literature to apply it to a NWP assimilation dataset over a large geographic and temporal scale with high resolution (13 km, hourly).

4. DISCUSSION AND CONCLUSIONS

The present paper described the creation of a 9 year (2006–2014), 13 km hourly dataset of estimated wind speeds and wind power at 80 m AGL, with rotor diameter of 100 m. The dataset contains the wind speed, density, temperature, clouds, precipitation at 80 m AGL and their rotor equivalent counterparts. The REWS with directional shear was the main focus of the paper. We demonstrated that the REWS does not alter the well known locations of high wind resource; however, the

Wind Energ. 2016; **19**:1687–1697 © 2015 The Authors. *Wind Energy* published by John Wiley & Sons, Ltd.
DOI: 10.1002/we

mean wind speeds and capacity factors are found to be lower than their hub height counterparts, as well as the NREL/AWS resource mapping. In addition, we use an icing constraint that is not present in the NREL/AWS resource mapping. There continues to be a significant lack of data on shutdowns due to icing of wind turbines.

The lower mean wind speeds and capacity factors compared with the NREL/AWS mapping could be caused by a number of factors. First, the lower spatial resolution of the current dataset (13 km) versus the NREL/AWS map (2 km) results in a coarser description of slopes, which will lead to a decrease in the speed up effects that can be created in steep terrain. Second, the longer time series used to create the dataset compared with the NREL/AWS map will result in the incorporation of more variability of wind speed changes (inter-annual variability) that could lower the relative average. Finally, the current dataset is based upon the analysis fields of a formerly operation NWP model, while the NREL/AWS dataset was created with a specific model for wind resource mapping. The difference in these models can alter the estimated wind speeds at 80 m AGL.

The dataset has some advantages compared with the NREL/AWS resource mapping. First, it estimates power potential using appropriate turbines for the resource region. Secondly, it incorporates the REWS, thereby including more information across the rotor swept area. Thirdly, it has a long time series with an analysis field that remained largely the same over the whole time period. Finally, it covers a larger geographic area, including much of Canada, some of northern Mexico and significant offshore areas. The main limitation is that it is a coarser resolution than the NREL/AWS resource mapping.

Figure 4 showed the correlation between the estimated and actual wind speed at 100 m AGL at Washburn, TX over a 6 year period. The correlation is very good with a general high bias at low wind speeds (< 7 m s^{-1}) and low bias at high wind speeds. In Figure 4(b), a 7 day period is shown for Washburn, TX, and it can be seen that the analysis field follows the wind speeds accurately. It is clear that sometimes the wind speeds are not the same (hours 48–90); the estimated wind speeds are significantly lower than the measured wind speeds. Additionally, there are times when the model wind speed does mimic a ramp, but it is offset temporally by an hour or two. Both of these effects are partially explained by the resolution of the NWP model. Since the model data is a 13 km average and the measurements are at a point, the model will not always detect structures that are smaller than $\sim$20 km, thus if there is a localized thunderstorm in the vicinity of the tower, where the measurements are being taken, the wind speeds at the tower would be increased, but the model may not be significantly altered from the passing large scale weather structures. For the delay or early ramp events, the grid average cannot depict the exact arrival of wind ramps at a specific location within the 13 km cell. Thus, the wind can be measured earlier or later than the model estimates it.

The assimilation analysis wind speeds do show the same behaviour as the measured wind speed. It is not expected that the estimates and the measurements are in perfect alignment because there is measurement error as well as model error. Further, the model is a spatial average, not a point estimate, so that must be taken into consideration when comparing to measurements. We intend to dedicate a future paper to comparing the estimated wind speeds with many more towers, to better understand the behaviour of the model. A comparison of the wind power estimates with power data from real wind farms will be included in this analysis.

In Figure 5, we displayed the 9-year mean capacity factors, along with the difference between the REWS estimates and the hub height estimates. The main result is that the average changes due to vertical and directional shear in the plains is small over large time periods. The alteration due to vertical and directional shear is more pronounced over complex terrain and towards the east. One limitation of the current REWS formulation is the lack of turbulence, which can dramatically alter the power production at wind sites; particularly in the plains. We will address turbulence in an upcoming paper. The turbulence adds more complications to the REWS formulation, and it is insightful to break the differences into components, thus the present paper investigated the vertical and directional shear only. The REWS formulation does reduce the estimated average wind power potential by 1.56% over the entire contiguous USA, with some sites experiencing a reduction of 15.4%. The reduction could have impacts on the viability of wind farms in the south east and mountainous regions. The REWS is a function of rotor diameter; the larger the rotor swept area the greater the vertical shear can be, contrasted by the fact that the larger rotor swept area will be effected less by small scale turbulence. There will be a tradeoff between taller hub heights, larger rotor blades and the cost effectiveness of power production.

In the final figure of the paper, Figure 6, we showed the difference heat map for the Washburn, TX site for 2010. We showed this particular site because we had measurements; thus knew the behaviour of the model compared with the measurements. Additionally, the 9 year difference was only -0.6% compared with the hub height estimate. The Washburn, TX site has a measured average wind speed of 9.0 m s^{-1} between 2006 and 2011, making it a very good wind resource site. The heap map illustrates the true impact of the vertical shear; an alteration of the time series behaviour. It suggests that there is more power than the hub height would estimate at night and less during the day. This could be important because more electricity is currently needed in the day than at night. It also depicts that spring and fall has higher power potential than the hub height estimate would suggest. Interestingly, an annulus feature can be seen at sunrise and (less so) at sunset, which is probably related to a change in the planetary boundary layer height, causing an acceleration of wind speeds in the top half of the rotor swept area. For the sake of brevity, we only showed 2010 because each year showed the same behaviour. The higher wind power over the summer nights could be due to the low level jet approaching the top of the rotor swept area. Again, these values are spatial averages, so actual wind turbines and farms may experience different values within a grid cell.

The current paper has used the analysis field from an advanced weather assimilation model to show the effect of vertical and directional shear on wind speeds and power over a large geographic area and time period. The main conclusion is that the REWS, on average, reduces the power potential of wind resource sites, as well as altering the time series behaviour of the wind resource. The changes could result in modifications to the cost of electricity from wind farms, the siting of wind turbines and the value of complementary resources such as solar photovoltaic power. The current dataset required a large amount of research; however, the dataset highlights the need for further investigation. First, the incorporation of turbulence is important. The authors hope to address this in an upcoming publication. Second, the full power equation needs to be used in the formulation of power. The full equation could change the time series because of the way numerical weather models output hourly variables; generally, they use the integration period nearest the top of the hour, and hence the wind speed and air density can change significantly in the ensuing hour. Third, the dataset needs to be compared against numerous high quality measurements of wind speed and power: to validate the effects that are observed at turbines and to determine the general behaviour of the assimilation model in different geographic locations. At the time of writing, the authors did not have access to such data, but they endeavor to obtain some to perform such validation. Fourth, higher horizontal resolution need to be computed to investigate the effect of REWS over complex terrain. Finally, incorporating more turbine hub heights and rotor diameters is warranted to allow for comparison between designs.

ACKNOWLEDGEMENTS

The authors would like to thank J. Olson, A. Dunbar, J. Wilczak, Y. Xie, M. Marquis, C. Sosa, A. Sitler and A. Way for their helpful comments, discussions and recommendations for the study carried out in the present paper. The authors are thankful to the two anonymous reviewers for their helpful comments and feedback that improved the paper immensely. The work contained herein was funded by the Office of Oceanic and Atmospheric Research at the National Oceanic and Atmospheric Administration.

REFERENCES

1. Wiser R, Yang Z, Hand M, Hohmeyer O, Ineld D, Jensen PH, Nikolaev V, OÕMalley M, Sinden G, Zervos A. Wind Energy. In *IPCC Special Report on Renewable Energy Sources and Climate Change Mitigation*, Edenhofer O, Pichs-Madruga R, Sokona Y, Seyboth K, Matschoss P, Kadner S, Zwickel T, Eickemeier P, Hansen G, Schlomer S, von Stechow C (eds). Cambridge University Press: Cambridge, United Kingdom and New York, NY, USA, 2011; 209–211.
2. Energy Information Administration (EIA). 2004. *International energy outlook 2013*. Dep. of Energy, Washington, DC (Available at http://www.eia.gov/forecasts/ieo/pdf/0484(2013).pdf) (Accessed January 2014).
3. Lantz E, Hand M, Wiser R. *WREF 2012: The Past and Future Cost of Wind Energy*, 2012. World Renewable Energy Forum, NREL/CP-6A20-54526.
4. Potter CW, Lew D, McCaa J, Cheng S, Eichelberger S, Grimit E. Creating the Dataset for the Western Wind and Solar Integration Study (U.S.A.) *Wind Engineering* 2008; **32**: 325–338.
5. Bailey BH, McDonald SL, Bernadett DW, Markus MJ, Elsholz KV. *Wind Resource Assessment Handbook*, 1997. Report Subcontract No. TAT-5-15283-01, National Renewable Energy Laboratory.
6. Archer CL, Jacobson MZ. Evaluation of global wind power. *Journal of Geophysical Research* 2005; **110**: D12110.
7. Adams AS, Keith DW. Are global wind power resource estimates overstated? *Environmental Research Letters* 2013; **8**: 015021.
8. Archer CL, Jacobson MZ. Geographical and seasonal variability of the global practical wind resources. *Applied Geography* 2013; **45**: 119–130.
9. Hoogwijk M, De Vries B, Turkenburg W. Assessment of the global and regional geographical, technical and economic potential of onshore wind energy. *Energy Economics* 2004; **26**: 889–919.
10. Zhou Y, Luckow P, Smith SJ, Clarke L. Evaluation of global onshore wind energy potential and generation costs. *Environmental Science and Technology* 2012; **46**: 7857–7864.
11. Kaminsky F. Four probability densities (log-normal, gamma, Weibull, and Rayleigh) and their application to modelling average hourly wind speed. *Proceedings of International Solar Energy Society Conference*, 1977; 19.6–19.10.
12. Weisser D. A wind energy analysis of Grenada: an estimation using the Weibull density function. *Renew. Energy* 2003; **28**: 1803–1812.
13. Jowder F. Weibull and Rayleigh distribution functions of wind speeds in Kingdom of Bahrain. *Wind Engineering* 2006; **30**: 439–445.
14. Tar K. Some statistical characteristics of monthly average wind speed at various heights. *Renewable and Sustainable Energy Reviews* 2008; **12**: 1712–1724.

15. Carta JA, Ramírez P Velázquez. A review of wind speed probability distributions used in wind energy analysis: case studies in the Canary Islands. *Renewable and Sustainable Energy Reviews* 2009; **13**: 933–955.
16. Chellali F, Khellaf A, Belouchrani A, Khanniche R. A comparison between wind speed distributions derived from the maximum entropy principle and Weibull distribution. Case of study; six regions of Algeria. *Renewable and Sustainable Energy Reviews* 2012; **16**: 379–385.
17. Zhou Y, Smith SJ. Spatial and temporal patterns of global onshore wind speed distributions. *Environmental Research Letters* 2013; **8**: 034029.
18. Wagner R, Antoniou I, Pedersen SM, Courtney MS, Jorgensen HE. The influence of the wind speed profile on wind turbine performance measurements. *Wind Energy* 2009; **12**: 348–362.
19. Choukulkar A, Pichugina Y, Clack CTM, Calhoun R, Banta R, Brewer A, Hardesty M. A new formulation for rotor equivalent wind speed for resource assessment and wind power forecasting. *Wind Energy* 2015. DOI: 10.1002/we.1929.
20. Wiser R, Bolinger M, *Wind Technologies Market Report*, Technical Report, Dep. of Energy, Washington, DC, 2013.
21. Benjamin SG, Grell GA, Brown JM, Smirnova TG, Bleck R. Mesoscale weather prediction with the RUC hybrid isentropic/terrain-following coordinate model. *Monthly Weather Reviews* 2004; **132**: 473–494.
22. Benjamin SG, Devenyi D, Weygandt SS, Brundage KJ, Brown JM, Grell G, Kim D, Schwartz BE, Smirnova TG, Smith TL, Manikin GS, 2004. An hourly assimilation/forecast cycle the RUC. *Monthly Weather Reviews*; **132**: 495–518.
23. Burton T, Sharpe D, Jenkins N, Bossanyi E. *Wind Energy Handbook*. John Wiley and Sons: Chichester England, 2001.
24. Pennock K, Clark K. *Updated Eastern Interconnect Wind Power Output and Forecasts for ERGIS*, 2012. Report Subcontract No. SR-5500-56616, National Renewable Energy Laboratory.
25. Draxl C, Clifton A, Hodge B-M, McCaa J. The wind integration national dataset (WIND) Toolkit. *Applied Energy* 2015; **151**: 355–366.
26. Betz A. *Wind-Energie und ihre ausnutzung durch Windmhlen*. Gottingen: Vandenhoeck, 1926.
27. International Electrotechnical Commission. *Wind turbines - Part 1: Design requirements, International Electrotechnical Commission, Geneva, Switzerland, 3rd ed.* 2005. IEC-61400-1.
28. Wharton S, Lundquist JK. Atmospheric stability affects wind turbine power collection. *Environmental Research Letters* 2012;
7: 014005.
29. Wharton S, Lundquist JK. Assessing atmospheric stability and its impacts on rotor-disk wind characteristics at an onshore wind farm. *Wind Energy* 2012; **15**: 525–546.
30. Clifton A, Kilcher L, Lundquist JK, Fleming P. Using machine learning to predict wind turbine power output. *Environmental Research Letters* 2013; **8**: 024009.
31. Derrick A, Atkinson N, Campbell I, Clerc A, Cronin J, Ely A, Feeney S, Hutton G, Lannic M, MacDonald M, Oram A, *Havsnäs Pilot Project Report on Cold Climate and High Hub Height*, Technical Report, Renewable Energy Systems Ltd and NV Nordisk Vindkraft, 2013.